
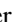



Effects of electron-electron interactions in the Yu-Shiba-Rusinov lattice model

Valerii Kachin ^{1,2}, Teemu Ojanen^{3,4}, Jose L. Lado ¹ and Timo Hyart ^{1,3}

¹*Department of Applied Physics, Aalto University, 02150 Espoo, Finland*

²*Faculty of Mathematics, Informatics and Mechanics, University of Warsaw, Banacha 2, 02-097, Poland*

³*Computational Physics Laboratory, Physics Unit, Faculty of Engineering and Natural Sciences, Tampere University, FI-33014 Tampere, Finland*

⁴*Helsinki Institute of Physics P.O. Box 64, FI-00014, Finland*



(Received 19 August 2022; revised 12 May 2023; accepted 12 May 2023; published 25 May 2023)

In two-dimensional superconductors, Yu-Shiba-Rusinov bound states, induced by the magnetic impurities, extend over long distances giving rise to a long-range hopping model supporting a large number of topological phases with distinct Chern numbers. Here, we study how the electron-electron interactions affect, on a mean-field level, the selection of the realized Chern numbers and the magnitudes of the topological energy gaps in this model. We find that, in the case of an individual choice of the model parameters, the interactions can enhance or reduce the topological gap as well as cause topological phase transitions because of the complex interplay of superconductivity, magnetism, and the large spatial extent of the Yu-Shiba-Rusinov states. By sampling a large number of realizations of Yu-Shiba-Rusinov lattice models with different model parameters, we show that, statistically, the interactions have no effect on the realized Chern numbers and typical magnitudes of the topological gaps. However, the interactions substantially increase the likelihood of the largest topological gaps in the tails of the energy gap distribution in comparison to the noninteracting case.

DOI: [10.1103/PhysRevB.107.174522](https://doi.org/10.1103/PhysRevB.107.174522)

I. INTRODUCTION

Magnetic impurities in conventional and nonmagnetic impurities in unconventional superconductors give rise to Yu-Shiba-Rusinov bound states, which were studied extensively both theoretically and experimentally [1–7]. An important property of these states in two-dimensional systems, as well as in three-dimensional layered structures, anisotropic systems, and systems supporting surface states, is that they spatially extend over long distances [5,6,8–13]. Therefore, in the presence of impurity chains and lattices, the coherent overlapping impurity states can give rise to long-range hopping models and topological superconductivity [14–18].

The one-dimensional magnetic adatom chains are theoretically predicted to support Majorana zero modes localized at the end of the chain [14–16,19–24] and promising signatures were experimentally observed [25–29]. These observations attracted significant interest in the quantum computing community because the non-Abelian braiding statistics of the Majorana zero modes. In particular, they can be utilized in topological quantum computing and when the quantum information stored in the Majorana qubits is protected from local sources of noise [30,31]. Although most of the braiding proposals were developed for Majorana nanowires [31], different methods for manipulating the quantum information in Yu-Shiba-Rusinov chains are also currently being explored [32–34]. Also the identification of Majorana zero modes from other low-energy bound states remains an active field of research [35,36].

The case of a two-dimensional Yu-Shiba-Rusinov lattice is theoretically even more interesting [17,37–45]. In this case the hybridization of the Yu-Shiba-Rusinov states gives rise

a rich phase diagram containing a large number of different topological phases [17,39–41]. These topological phases are described by an integer-valued Chern number C [46], which determines the number of chiral Majorana edge modes (see Fig. 1) and value of the quantized thermal conductance [47,48]. So far the quantization of the thermal conductance in superconductors has remained elusive, but recent experiments show promising signatures of the Majorana edge modes in the local density of states (LDOS) data measured via the scanning tunneling spectroscopy techniques [49–52], and unbiased methods for identifying the Chern number from LDOS are currently under development [53–57]. Therefore, there are reasons to be optimistic that the topological phase diagram of the Yu-Shiba-Rusinov lattice system can be probed also experimentally in the near future.

The rich topological phase diagram of the Yu-Shiba-Rusinov lattice model [17,39–41] calls for a detailed theoretical analysis of the different factors that may play an important role in the selection of the topological phases, which are actually realized in the experiments. So far most of the studies mainly focused on extrinsic factors and it is known, for example, that in the presence of strong disorder only the $C = 0$ and $C = 1$ phases survive [58], out of the dozens of topologically distinct phases appearing in a clean system [17,41]. Here, we study an important intrinsic factor which is present also in the highest quality samples: the effect of electron-electron interactions. We may expect that they lead to competing effects. On one hand, the interactions favor states with large energy gaps to lower the free energy in the many-particle systems. On the other hand, the phases with large Chern numbers are most fragile to the effects of the perturbations because they arise from a complex interplay of the superconductivity,

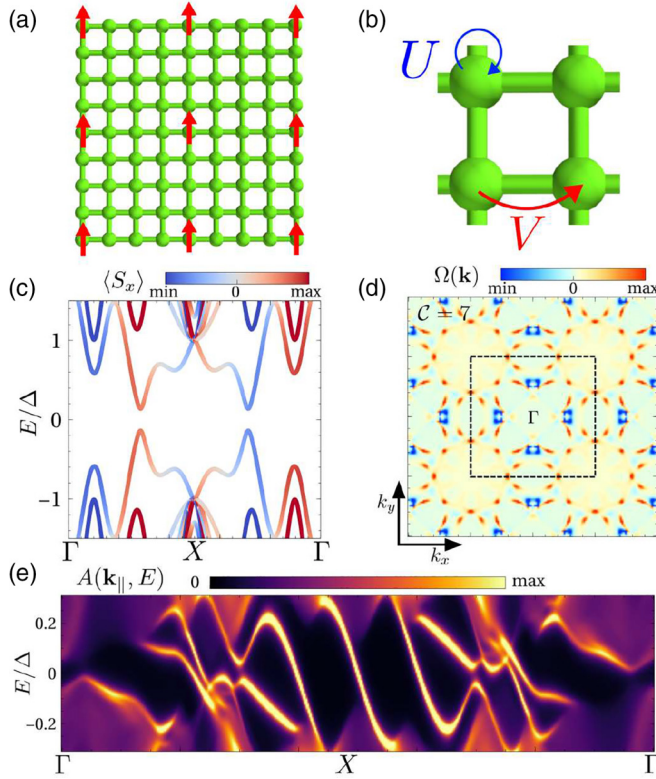


FIG. 1. (a) Schematic representation of the Yu-Shiba-Rusinov lattice consisting of a square lattice of magnetic impurities with a lattice constant $a = 4$ placed on the top of a two-dimensional superconductor. (b) The electron-electron interaction terms considered in this work are the onsite U and the nearest-neighbor interaction V . (c) Bulk band structure and (d) Berry curvature $\Omega(\mathbf{k})$ for a Yu-Shiba-Rusinov lattice with $a = 8$, $\nu = 0.1$, $J = 2.272t$, $\alpha = 0.113t$, $\Delta = 0.06t$, $U = -0.37t$, realizing a topological phase with Chern number $C = 7$. (e) The surface density of states for the same model parameters featuring seven chiral Majorana edge modes.

magnetism, and large spatial extent of the Yu-Shiba-Rusinov states. In particular, the increase of the energy gap leads to a shorter coherence length decreasing the long-range coupling between the Shiba states, which is essential for realizing large Chern numbers. Therefore, the interactions could favor the phases with small Chern numbers, where it is easier to open sizable energy gaps. But, in order that the interactions could result in a change of the Chern number from a large to a small value the system, in the absence of first-order transitions, has to undergo a series of energy gap closings. Thus, the interactions can also lead to lowering of the energy gaps. We show that these competing tendencies in this type of complicated system supporting dozens of topologically distinct phases lead to rather surprising statistical effects. By sampling a large number of realizations of Yu-Shiba-Rusinov lattice models with different model parameters, we show that, statistically, the interactions have practically no effect on the realized Chern numbers and typical magnitudes of the topological gaps. However, the interactions substantially enhance the likelihood of the rare realizations of large topological gaps in the tails of the energy gap distribution in comparison to the noninteracting case.

II. MODEL

The Hamiltonian of the system takes the form

$$\mathcal{H} = \mathcal{H}_{\text{kin}} + \mathcal{H}_R + \mathcal{H}_J + \mathcal{H}_{\text{SC}}, \quad (1)$$

where \mathcal{H}_{kin} describes the nearest-neighbor hopping

$$\mathcal{H}_{\text{kin}} = t \sum_{\langle ij \rangle} c_{i,s}^\dagger c_{j,s}, \quad (2)$$

\mathcal{H}_R is the Rashba spin-orbit coupling

$$\mathcal{H}_R = i\alpha \sum_{\langle ij \rangle} \hat{z} \cdot (\mathbf{d}_{ij} \times \boldsymbol{\sigma}_{s,s'}) c_{i,s}^\dagger c_{j,s'}, \quad (3)$$

\mathcal{H}_J is the magnetic exchange coupling induced by the impurities

$$\mathcal{H}_J = J \sum_{i \in \text{imp}} \sigma_{s,s'}^z c_{i,s}^\dagger c_{i,s'}, \quad (4)$$

and \mathcal{H}_{SC} describes the superconducting pairing

$$\mathcal{H}_{\text{SC}} = \Delta \sum_i c_{i,\uparrow}^\dagger c_{i,\downarrow}^\dagger + \text{H.c.} \quad (5)$$

Here $c_{i,s}^\dagger$ is the creation operator for an electron in site i and spin s , $\mathbf{d}_{ij} = \mathbf{r}_i - \mathbf{r}_j$, and $i \in \text{imp}$ indicates that the summation is over the impurity sites. We assume that the impurity sites form a square lattice with lattice constant of a , as shown in Fig. 1(a).

The many-body interactions are included by means of an local U and nearest-neighbor V density-density interaction [see Fig. 1(b)] of the form

$$\mathcal{H}_{\text{int}} = \mathcal{H}_U + \mathcal{H}_V, \quad (6)$$

$$\mathcal{H}_U = U \sum_i c_{i,\uparrow}^\dagger c_{i,\uparrow} c_{i,\downarrow}^\dagger c_{i,\downarrow}, \quad (7)$$

$$\mathcal{H}_V = V \sum_{\langle ij \rangle} \left(\sum_s c_{i,s}^\dagger c_{i,s} \right) \left(\sum_{s'} c_{j,s'}^\dagger c_{j,s'} \right). \quad (8)$$

The Hamiltonian is solved at the mean-field level $\mathcal{H}_{\text{int}} \approx \mathcal{H}_{\text{int}}^{\text{MF}}$ including all the bilinear contractions of the mean-field

$$\mathcal{H}_{\text{int}}^{\text{MF}} = \sum_{i,j,s,s'} \chi_{i,j}^{s,s'} c_{i,s}^\dagger c_{j,s'} + \sum_{i,j,s,s'} \xi_{i,j}^{s,s'} c_{i,s}^\dagger c_{j,s'} + \text{H.c.}, \quad (9)$$

giving rise to hopping, pairing, chemical potential, and spin-orbit coupling renormalization [59]. We elaborate now on the different terms that emerge. Local interactions involving $c_{i,\uparrow}^\dagger c_{i,\uparrow} c_{i,\downarrow}^\dagger c_{i,\downarrow}$ give rise to chemical potential, collinear magnetic $\langle c_{i,\uparrow}^\dagger c_{i,\uparrow} \rangle c_{i,\downarrow}^\dagger c_{i,\downarrow}$, noncollinear magnetic $\langle c_{i,\uparrow}^\dagger c_{i,\downarrow} \rangle c_{i,\downarrow}^\dagger c_{i,\uparrow}$, and s -wave superconducting $\langle c_{i,\uparrow}^\dagger c_{i,\downarrow} \rangle c_{i,\uparrow} c_{i,\downarrow}$ terms or their renormalization (including all combinations). First-neighbor interactions $(\sum_s c_{i,s}^\dagger c_{i,s})(\sum_{s'} c_{j,s'}^\dagger c_{j,s'})$ lead to chemical potential, collinear magnetic $\langle c_{i,\uparrow}^\dagger c_{i,\uparrow} \rangle c_{j,\downarrow}^\dagger c_{j,\downarrow}$, hopping $\langle c_{i,s}^\dagger c_{j,s} \rangle c_{j,s}^\dagger c_{i,s}$, spin-flip hopping including synthetic spin-orbit $\langle c_{i,\uparrow}^\dagger c_{j,\downarrow} \rangle c_{i,\downarrow}^\dagger c_{j,\uparrow}$, and singlet and triplet superconducting terms $\langle c_{i,s}^\dagger c_{j,s'}^\dagger \rangle c_{i,s} c_{j,s'}$, including all combinations.

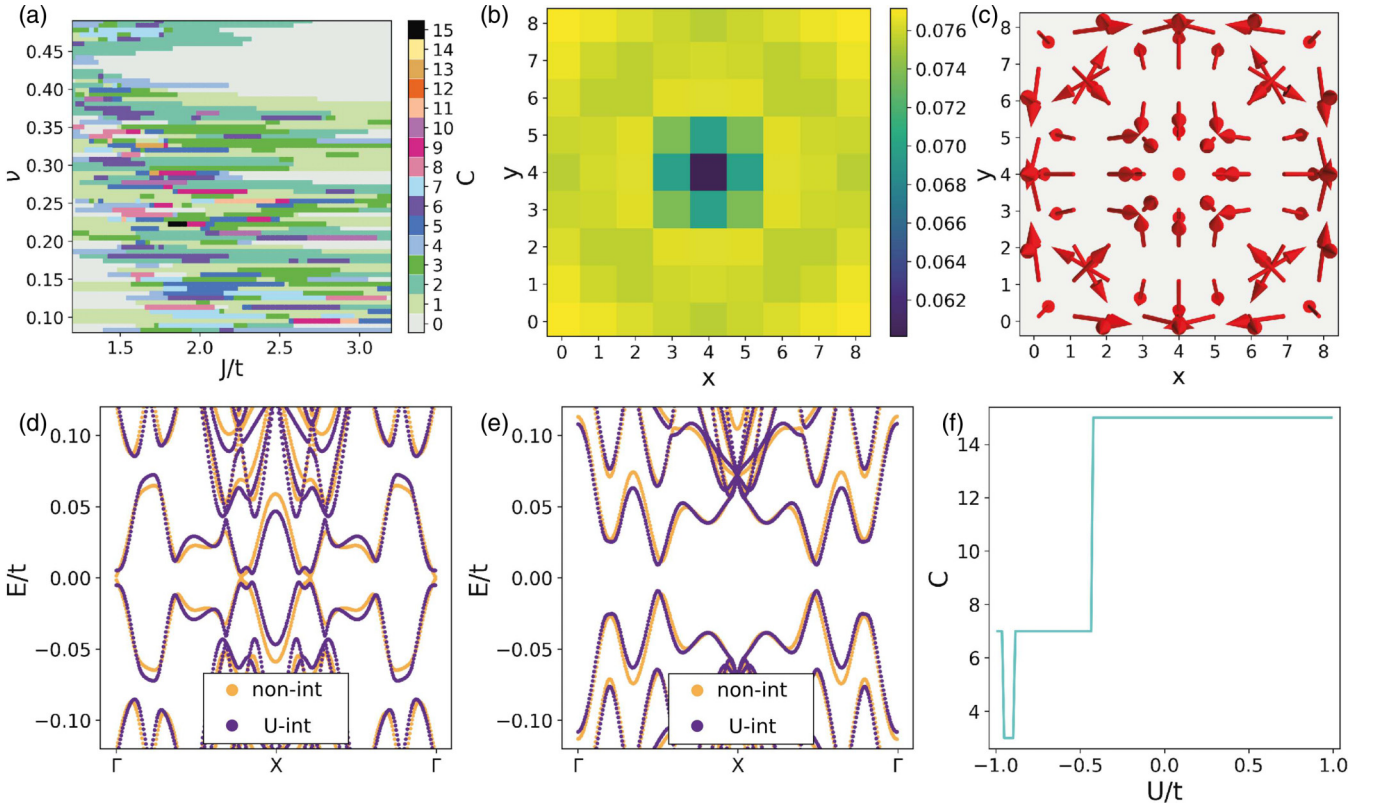


FIG. 2. (a) Phase diagram of the noninteracting model as a function of filling ν and the exchange interaction J for $\alpha = 0.1t$ and $\Delta = 0.06t$. (b,c) Illustrations of effects of interactions on the mean-field superconductivity and magnetization, respectively. The magnetic impurity is located at the center of the unit cell. The parameters are (b) $\nu = 0.101$, $J = 2.433t$, $\alpha = 0.112t$, $\Delta = 0.054t$, $U = -0.702t$ and (c) $\nu = 0.115$, $J = 2.172t$, $\alpha = 0.117t$, $\Delta = 0.052t$, $U = 0.644t$, $V = 0.012t$. (d), (e) Examples of spectra where the interactions enhance the gap and reduce the gap, respectively. The parameters are (d) $\nu = 0.115$, $J = 2.172t$, $\alpha = 0.117t$, $\Delta = 0.052t$, $U = 0.644t$, $V = 0.012t$ and (e) $\nu = 0.1$, $J = 2.272t$, $\alpha = 0.113t$, $\Delta = 0.06t$, $U = -0.37t$. (f) Illustration of topological phase transitions as a function of interaction strength U for $\nu = 0.1$, $J = 2.272t$, $\alpha = 0.113t$, $\Delta = 0.06$. In all cases we assume a square lattice of impurities with a lattice constant $a = 8$.

Our mean-field calculations include all the different contractions of two-field operators in a fully self-consistent manner, capturing all those effects on the same footing. By studying separately the cases where only U is present (U -interacting case) and both U and V are present (UV -interacting case) we can also get some idea how the range of the interactions affects the results. The self-consistent calculations are performed at fixed filling of the normal state $\nu \in [0, 1]$. Since we assume everywhere that $\Delta \ll t$, ν also approximately describes the filling of the bands in the presence of superconductivity. We compute the Chern number numerically using a gauge-invariant description of Chern number associated with the Berry connection defined on a discretized Brillouin zone [60] (see the Appendix for more details). Importantly, because the sign of the Chern number is not important for our analysis, everywhere in the paper we denote with C the absolute value of the Chern number.

For concreteness, we show in Fig. 1(c) the electronic structure of a specific example of the Yu-Shiba-Rusinov lattice model. The corresponding Berry curvature distribution $\Omega(\mathbf{k})$ is shown in Fig. 1(d) and by integrating $\Omega(\mathbf{k})$ over the Brillouin zone we obtain a Chern number $C = 7$. As a consequence of $C = 7$, the spectral function in a semi-infinite geometry features seven chiral edge modes crossing the energy gap, as shown in Fig. 1(e).

III. EFFECTS OF INTERACTIONS ON INDIVIDUAL REALIZATIONS

In the limit when $\Delta \ll t$ and the impurity lattice constant satisfies $a \gg 1$, the noninteracting model of Eqs. (1) to (5) supports a rich topological phase diagram as a function of model parameters [17,39,41]. In Fig. 2(a) we show a representative phase diagram for $a = 8$ as a function of filling ν and the exchange interaction J for $\alpha = 0.1t$ and $\Delta = 0.06t$. It contains topological phases with Chern numbers ranging from 0 to 15 arising due to the long-range coupling between the Yu-Shiba-Rusinov states [17]. The high Chern number topological phases originate from rather peculiar situations where the longer-range couplings between the Shiba states are larger than the shorter-range couplings, and therefore they cover only small areas of the parameter space [see Fig. 2(a)]. This also means that the phases with large C are quite fragile against the effects of perturbations and, for example, in the presence of strong disorder only the $C = 0$ and $C = 1$ phases survive [58].

The electron-electron interactions can influence the topological phases because they can modify the spatial profiles of the mean fields. We find that in the presence of interactions the superconducting mean field is modulated with the period a of the magnetic impurities. A representative example of

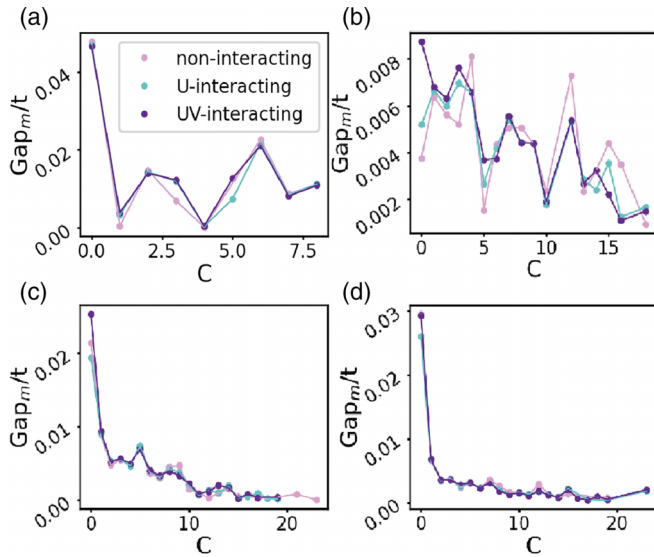


FIG. 3. Median energy gap values for different values of C in the noninteracting, U -interacting, UV -interacting cases for different impurity lattice constants (a) $a = 2$, (b) $a = 4$, (c) $a = 6$, and (d) $a = 8$. The sampling of the model parameters is described in the main text.

a single unit cell of the impurity lattice with the magnetic impurity located at the center of it is shown in Fig. 2(b). In the case of magnetization, the interactions do not only modify the magnitude of the mean field, but also lead to an appearance of magnetization textures where the direction of the magnetization varies within the unit cell [see Fig. 2(c)]. We find that these effects can both enhance and reduce the topological energy gap and even cause topological phase transitions [see Figs. 2(d) to 2(f)]. Therefore, we conclude that the interaction effects can play an important role in the determination of the topological phase and the magnitude of the topological gap in the case of individual samples.

IV. STATISTICAL EFFECTS OF INTERACTIONS

The model parameters are rarely known accurately in experiments. Therefore, rather than studying the system for specific model parameters, it is important to establish the statistical effects of the interactions on the existence of the topological phases with high C and for the magnitudes of the corresponding energy gaps. For this purpose we collected statistics of the gap sizes and Chern numbers for 50 000 sets of model parameters in impurity lattices with lattice constant $a =: 2, 4, 6, 8$. In the sampling we use common ranges $v \in [0.1, 0.45]$, $\alpha \in t[0.08, 0.12]$, $\Delta \in t[0.048, 0.072]$, $U \in t[-1.0, 1.0]$, and $V \in t[-0.5, 0.5]$, whereas the sampling of J for each a is chosen so that the topological phase diagrams contain a large number of topologically distinct phases. We use $J \in t[0.76, 1.2]$ for $a = 2$, $J \in t[1.4, 2.1]$ for $a = 4$, and $J \in t[1.8, 2.7]$ for $a = 6$ and $a = 8$.

In Fig. 3 we show the median energy gap values for different values of C in the noninteracting, U -interacting, and UV -interacting cases for different impurity lattice constants. The median gap values oscillate as a function of C , but there is also a general tendency for the energy gaps to become

smaller and smaller with increasing values of C . Importantly, we find that the median energy gaps have remarkably similar magnitudes and dependence on C in the noninteracting, U -interacting, and UV -interacting cases (see Fig. 3). This suggests that the interactions are not statistically relevant in the determination of the topological phases and magnitudes of the topological gaps within the quite large range of interaction strengths considered. We believe that the interval of the electron-electron interaction strengths is sufficiently large to draw reliable conclusions because the interactions are screened by the superconductor and therefore larger interaction strengths are unlikely to occur in the realization of the Shiba lattice models.

The median gap values of course give only partial information about the distribution of the gap values and it could be possible that the interactions still affect the shape of this distribution. In Fig. 4 we plot the whole statistical distribution of the gap values in the cases of small, intermediate, and large Chern numbers. The distributions are practically identical in the noninteracting, U -interacting, and UV -interacting cases in the case of small gap sizes. Since the distribution function decays approximately exponentially with the increasing energy gap values (see Fig. 4) the small gap values occur much more commonly than the large ones, so that the typical gap sizes are indeed the same in the interacting and noninteracting cases. However, the rare events corresponding to large topological gaps show a drastically different phenomenology. As shown in Fig. 4, for all the Chern numbers interactions substantially increase the probability of the largest topological gaps. In that regime, the noninteracting gap distribution decreases much faster than exponentially when the energy gap values approach the upper bound of the gap values of the corresponding Chern numbers that can be realized in the noninteracting Yu-Shiba-Rusinov model. In the presence of interactions, the number of samples exhibiting a large topological gap becomes much larger than in the noninteracting case, demonstrating that the interactions play an important role in the case of these rare events.

V. CONCLUSION AND DISCUSSION

To conclude, we studied the effects of electron-electron interactions in the two-dimensional Yu-Shiba-Rusinov lattice model on the mean-field level and our results show that the interactions can enhance or reduce the topological gap as well as cause topological phase transitions. We showed that, statistically, the distributions of the Chern numbers and the topological energy gaps in the noninteracting and interacting cases are approximately the same for the most common realizations where the energy gaps are reasonably small. Interestingly, we find that the probability of rare realizations with large energy gaps, located at the tails of statistical distributions, are strongly enhanced by interactions. Such realizations are challenging to find experimentally due to their small likelihood, but they would be the most suitable ones for the applications of topological superconductivity.

Our results provide also a starting point for studies of more subtle correlation effects in Shiba lattice models. We believe that the consideration of the interaction effects beyond the mean-field theory, such as quantum fluctuations

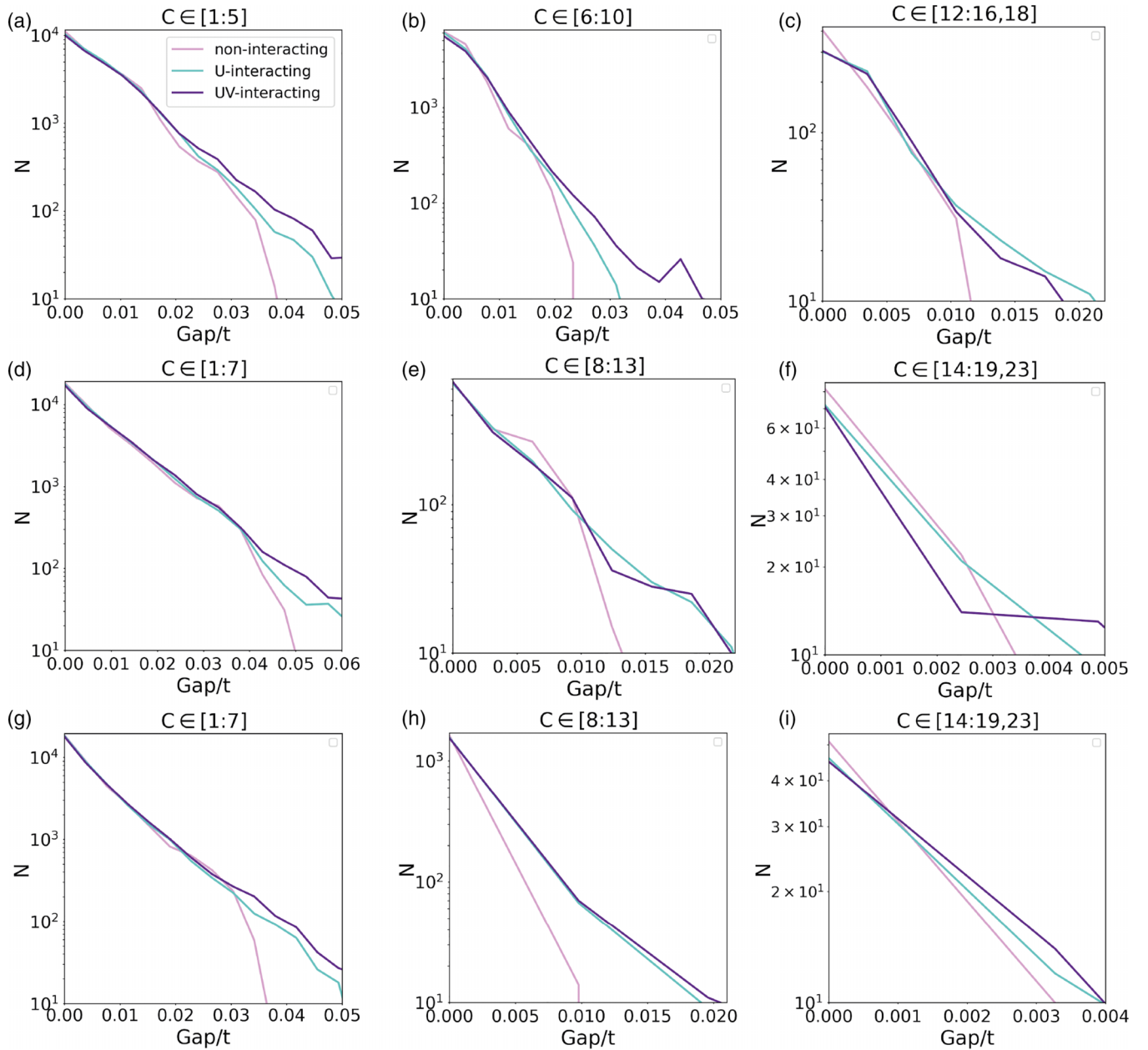


FIG. 4. Statistical distributions of the energy gap values in the noninteracting, U -interacting, and UV -interacting cases for different lattice constants (a)–(c) $a = 4$, (d)–(f) $a = 6$, and (g)–(i) $a = 8$, respectively. The statistical distributions are nearly identical in all cases in the regime of small energy gaps. In contrast, interactions substantially modify the tails of the distributions increasing the likelihood of large topological gaps.

[61,62] and Kondo physics [63], might be worth pursuing because these models may support unprecedented many-particle phenomenology thanks to the interplay of superconductivity, magnetism, high Chern numbers, and the large spatial extent of the Yu-Shiba-Rusinov states. In particular, the interactions in this type of high-Chern number quasi-flat-band system could lead to fractionalization and more exotic non-Abelian phases.

However, the current problem would pose a great challenge for most of the methods developed for calculating the properties of low-dimensional interacting systems. The biggest challenge in the exact diagonalization, tensor-network [64], and neural-network [65] calculations would be the large

supercell. We note that a similar limitation emerges also in moiré systems, but there the projection of interactions on a single or few low-energy bands allows to get a reduced effective model [66,67]. An alternative strategy would be to use a dynamical mean-field theory [68] or GW methodology [69] to obtain a more accurate picture of the renormalization of the electronic structure due to interactions. Finally, we point out that, because the interactions in our calculations do not lead to spontaneous breaking of symmetries, it is also possible that the mean-field calculations provide a reasonably good description of the many-body states [70].

Many of the current realizations of Yu-Shiba-Rusinov states are in multiorbital systems. In this case, our results can

still be applicable for a dilute lattice of adatoms because, in this case, the hybridization of the Shiba states is weak so that the low-energy Shiba bands are expected to originate dominantly from one of the orbitals. Nevertheless, ultimately, the realistic modeling of the interaction effects in Yu-Shiba-Rusinov lattices should be based on a multiorbital Wannier Hamiltonian extracted from first-principles density functional theory calculations, together with a multiorbital model for the magnetic impurity with orbital-dependent exchange couplings.

ACKNOWLEDGMENTS

We acknowledge the computational resources provided by the Aalto Science-IT project. We acknowledge financial support from the Academy of Finland Projects No. 331094, No. 331342, and No. 336243, and the Jane and Aatos Erkkö Foundation.

APPENDIX: MULTIBAND CALCULATION OF THE CHERN NUMBER

The conventional definition of the Berry curvature requires the computation of a derivative of the wave functions. The gauge degree of freedom of the eigenstates, giving rise to a different random phase for each \mathbf{k} -point, causes a problem when attempting to compute derivatives numerically. This problem is avoided in the Wilson loop formalism in a discretized \mathbf{k} -mesh. We denote the eigenstates and eigenenergies of a Bogoliubov–de Gennes Hamiltonian $H_{\mathbf{k}}$ with $|\Psi_{\mathbf{k}}^{\alpha}\rangle$ and $\epsilon_{\mathbf{k}}^{\alpha}$, respectively.

The Berry phase of the occupied states for a closed loop of discrete \mathbf{k} -points $\mathbf{k}_1, \mathbf{k}_2, \dots, \mathbf{k}_n, \mathbf{k}_1$ can be computed as

$$\phi_A = \arg[\det(R)], \quad (\text{A1})$$

where

$$R = R_{1,2}R_{2,3}, \dots, R_{n,1}, \quad (\text{A2})$$

$$R_{n,n+1}^{\alpha,\beta} = \langle \Psi_{\mathbf{k}_n}^{\alpha} | \Psi_{\mathbf{k}_{n+1}}^{\beta} \rangle, \quad (\text{A3})$$

and α, β runs over the negative energy states $\epsilon_{\mathbf{k}}^{\alpha,\beta} < 0$. It is worth noting that this definition is gauge invariant under any local non-Abelian transformation in the manifold of occupied states. This implies that the random phases and mixing of the eigenstates are not influencing the numerical calculation of the Berry phase. The previous formula can be derived by recalling that, in a diagonal multiband scenario, the total Berry phase is the sum of the phases of the diagonal components of R , which in a matrix-invariant form can be written as Eq. (A1). The Berry phase ϕ_A is related to the Berry curvature $\Omega(\mathbf{k})$ as

$$\phi_A = \int_A \Omega(\mathbf{k}) d^2\mathbf{k}, \quad (\text{A4})$$

where A is the area of the \mathbf{k} -space encircled by the Berry phase path. Therefore, by applying Eq. (A1) to an arbitrarily small path surrounding each point \mathbf{k} , the Berry curvature can be computed as

$$\Omega(\mathbf{k}) = \lim_{A \rightarrow 0} \phi_A / A, \quad (\text{A5})$$

with A an infinitesimally small area. Thus, an accurate numerical calculation of the Berry curvature requires a dense mesh. Finally, the Chern number can be computed by integrating the Berry curvature in the full Brillouin zone

$$C = \frac{1}{2\pi} \int_{BZ} \Omega(\mathbf{k}) d^2\mathbf{k}. \quad (\text{A6})$$

The calculation of the Chern number was numerically implemented using the PYQUILA library [59].

-
- [1] L. Yu, Bound state in superconductors with paramagnetic impurities, *Acta Phys. Sin* **21**, 75 (1965).
 - [2] H. Shiba, Classical spins in superconductors, *Prog. Theor. Phys.* **40**, 435 (1968).
 - [3] A. Rusinov, Superconductivity near a paramagnetic impurity, *Soviet Journal of Experimental and Theoretical Physics Letters* **9**, 85 (1969).
 - [4] A. V. Balatsky, I. Vekhter, and J.-X. Zhu, Impurity-induced states in conventional and unconventional superconductors, *Rev. Mod. Phys.* **78**, 373 (2006).
 - [5] G. C. Ménard, S. Guissart, C. Brun, S. Pons, V. S. Stolyarov, F. Debontridder, M. V. Leclerc, E. Janod, L. Cario, D. Roditchev *et al.*, Coherent long-range magnetic bound states in a superconductor, *Nat. Phys.* **11**, 1013 (2015).
 - [6] E. Cortés-del Río, J. L. Lado, V. Cherkov, P. Mallet, J. Veuillen, J. C. Cuevas, J. M. Gómez-Rodríguez, J. Fernández-Rossier, and I. Brihuega, Observation of Yu–Shiba–Rusinov states in superconducting graphene, *Adv. Mater.* **33**, 2008113 (2021).
 - [7] S. Basak and A. Ptok, Shiba states in systems with density of states singularities, *Phys. Rev. B* **105**, 094204 (2022).
 - [8] M. Ruby, Y. Peng, F. von Oppen, B. W. Heinrich, and K. J. Franke, Orbital Picture of Yu–Shiba–Rusinov Multiplets, *Phys. Rev. Lett.* **117**, 186801 (2016).
 - [9] S. Kezilebieke, M. Dvorak, T. Ojanen, and P. Liljeroth, Coupled Yu–Shiba–Rusinov States in Molecular Dimers on NbSe₂, *Nano Lett.* **18**, 2311 (2018).
 - [10] E. Liebhaber, S. Acero González, R. Baba, G. Reecht, B. W. Heinrich, S. Rohlf, K. Rossnagel, F. von Oppen, and K. J. Franke, Yu–Shiba–Rusinov States in the Charge-Density Modulated Superconductor NbSe₂, *Nano Lett.* **20**, 339 (2020).
 - [11] L. Farinacci, G. Ahmadi, M. Ruby, G. Reecht, B. W. Heinrich, C. Czekelius, F. von Oppen, and K. J. Franke, Interfering Tunneling Paths through Magnetic Molecules on Superconductors: Asymmetries of Kondo and Yu–Shiba–Rusinov Resonances, *Phys. Rev. Lett.* **125**, 256805 (2020).
 - [12] H. Kim, L. Rózsa, D. Schreyer, E. Simon, and R. Wiesendanger, Long-range focusing of magnetic bound states in superconducting lanthanum, *Nat. Commun.* **11**, 4573 (2020).
 - [13] U. Thupakula, V. Perrin, A. Palacio-Morales, L. Cario, M. Aprili, P. Simon, and F. Massee, Coherent and Incoherent Tunneling into Yu–Shiba–Rusinov States Revealed by Atomic Scale Shot-Noise Spectroscopy, *Phys. Rev. Lett.* **128**, 247001 (2022).
 - [14] F. Pientka, L. I. Glazman, and F. von Oppen, Topological superconducting phase in helical Shiba chains, *Phys. Rev. B* **88**, 155420 (2013).

- [15] F. Pientka, L. I. Glazman, and F. von Oppen, Unconventional topological phase transitions in helical Shiba chains, *Phys. Rev. B* **89**, 180505(R) (2014).
- [16] P. M. R. Brydon, S. Das Sarma, H.-Y. Hui, and J. D. Sau, Topological Yu-Shiba-Rusinov chain from spin-orbit coupling, *Phys. Rev. B* **91**, 064505 (2015).
- [17] J. Röntynen and T. Ojanen, Topological Superconductivity and High Chern Numbers in 2D Ferromagnetic Shiba Lattices, *Phys. Rev. Lett.* **114**, 236803 (2015).
- [18] F. Küster, S. Brinker, S. Lounis, S. S. P. Parkin, and P. Sessi, Long range and highly tunable interaction between local spins coupled to a superconducting condensate, *Nat. Commun.* **12**, 6722 (2021).
- [19] T.-P. Choy, J. M. Edge, A. R. Akhmerov, and C. W. J. Beenakker, Majorana fermions emerging from magnetic nanoparticles on a superconductor without spin-orbit coupling, *Phys. Rev. B* **84**, 195442 (2011).
- [20] B. Braunecker and P. Simon, Interplay between Classical Magnetic Moments and Superconductivity in Quantum One-Dimensional Conductors: Toward a Self-Sustained Topological Majorana Phase, *Phys. Rev. Lett.* **111**, 147202 (2013).
- [21] J. Klinovaja, P. Stano, A. Yazdani, and D. Loss, Topological Superconductivity and Majorana Fermions in RKKY Systems, *Phys. Rev. Lett.* **111**, 186805 (2013).
- [22] M. M. Vazifeh and M. Franz, Self-Organized Topological State with Majorana Fermions, *Phys. Rev. Lett.* **111**, 206802 (2013).
- [23] G. Sharma and S. Tewari, Yu-Shiba-Rusinov states and topological superconductivity in Ising paired superconductors, *Phys. Rev. B* **94**, 094515 (2016).
- [24] J. F. Steiner, C. Mora, K. J. Franke, and F. von Oppen, Quantum Magnetism and Topological Superconductivity in Yu-Shiba-Rusinov Chains, *Phys. Rev. Lett.* **128**, 036801 (2022).
- [25] S. Nadj-Perge, I. K. Drozdov, J. Li, H. Chen, S. Jeon, J. Seo, A. H. MacDonald, B. A. Bernevig, and A. Yazdani, Observation of Majorana fermions in ferromagnetic atomic chains on a superconductor, *Science* **346**, 602 (2014).
- [26] M. Ruby, F. Pientka, Y. Peng, F. von Oppen, B. W. Heinrich, and K. J. Franke, End States and Subgap Structure in Proximity-Coupled Chains of Magnetic Adatoms, *Phys. Rev. Lett.* **115**, 197204 (2015).
- [27] H. Kim, A. Palacio-Morales, T. Posske, L. Rózsa, K. Palotás, L. Szunyogh, M. Thorwart, and R. Wiesendanger, Toward tailoring Majorana bound states in artificially constructed magnetic atom chains on elemental superconductors, *Sci. Adv.* **4**, eaar5251 (2018).
- [28] L. Schneider, P. Beck, T. Posske, D. Crawford, E. Mascot, S. Rachel, R. Wiesendanger, and J. Wiebe, Topological Shiba bands in artificial spin chains on superconductors, *Nat. Phys.* **17**, 943 (2021).
- [29] L. Schneider, P. Beck, J. Neuhaus-Steinmetz, L. Rózsa, T. Posske, J. Wiebe, and R. Wiesendanger, Precursors of Majorana modes and their length-dependent energy oscillations probed at both ends of atomic Shiba chains, *Nat. Nanotechnol.* **17**, 384 (2022).
- [30] C. Nayak, S. H. Simon, A. Stern, M. Freedman, and S. Das Sarma, Non-Abelian anyons and topological quantum computation, *Rev. Mod. Phys.* **80**, 1083 (2008).
- [31] C. W. J. Beenakker, Search for non-Abelian Majorana braiding statistics in superconductors, *SciPost Phys. Lect. Notes* **15** (2020).
- [32] J. Li, T. Neupert, B. A. Bernevig, and A. Yazdani, Manipulating Majorana zero modes on atomic rings with an external magnetic field, *Nat. Commun.* **7**, 10395 (2016).
- [33] A. Kreisel, T. Hyart, and B. Rosenow, Tunable topological states hosted by unconventional superconductors with adatoms, *Phys. Rev. Res.* **3**, 033049 (2021).
- [34] A. Mishra, P. Simon, T. Hyart, and M. Trif, Yu-Shiba-Rusinov Qubit, *PRX Quantum* **2**, 040347 (2021).
- [35] F. Küster, S. Brinker, R. Hess, D. Loss, S. S. P. Parkin, J. Klinovaja, S. Lounis, and P. Sessi, Non-Majorana modes in diluted spin chains proximitized to a superconductor, *Proc. Natl. Acad. Sci. USA* **119**, e2210589119 (2022).
- [36] L. Schneider, P. Beck, L. Rózsa, T. Posske, J. Wiebe, and R. Wiesendanger, Testing the topological nature of end states in antiferromagnetic atomic chains on superconductors, [arXiv:2211.00561](https://arxiv.org/abs/2211.00561).
- [37] S. Nakosai, Y. Tanaka, and N. Nagaosa, Two-dimensional p-wave superconducting states with magnetic moments on a conventional s-wave superconductor, *Phys. Rev. B* **88**, 180503(R) (2013).
- [38] L. Kimme, T. Hyart, and B. Rosenow, Symmetry-protected topological invariant and Majorana impurity states in time-reversal-invariant superconductors, *Phys. Rev. B* **91**, 220501(R) (2015).
- [39] J. Li, T. Neupert, Z. Wang, A. H. MacDonald, A. Yazdani, and B. A. Bernevig, Two-dimensional chiral topological superconductivity in Shiba lattices, *Nat. Commun.* **7**, 12297 (2016).
- [40] L. Kimme and T. Hyart, Existence of zero-energy impurity states in different classes of topological insulators and superconductors and their relation to topological phase transitions, *Phys. Rev. B* **93**, 035134 (2016).
- [41] J. Röntynen and T. Ojanen, Chern mosaic: Topology of chiral superconductivity on ferromagnetic adatom lattices, *Phys. Rev. B* **93**, 094521 (2016).
- [42] A. Ptok, S. Głodzik, and T. Domański, Yu-Shiba-Rusinov states of impurities in a triangular lattice of NbSe₂ with spin-orbit coupling, *Phys. Rev. B* **96**, 184425 (2017).
- [43] O. Viyuela, L. Fu, and M. A. Martin-Delgado, Chiral Topological Superconductors Enhanced by Long-Range Interactions, *Phys. Rev. Lett.* **120**, 017001 (2018).
- [44] S. Głodzik and T. Ojanen, Engineering nodal topological phases in Ising superconductors by magnetic superstructures, *New J. Phys.* **22**, 013022 (2020).
- [45] M. Khosravian and J. L. Lado, Impurity-induced excitations in twisted topological van der Waals superconductors, *Phys. Rev. Mater.* **6**, 094010 (2022).
- [46] D. J. Thouless, M. Kohmoto, M. P. Nightingale, and M. den Nijs, Quantized Hall Conductance in a Two-Dimensional Periodic Potential, *Phys. Rev. Lett.* **49**, 405 (1982).
- [47] N. Read and D. Green, Paired states of fermions in two dimensions with breaking of parity and time-reversal symmetries and the fractional quantum Hall effect, *Phys. Rev. B* **61**, 10267 (2000).
- [48] T. Senthil and M. P. A. Fisher, Quasiparticle localization in superconductors with spin-orbit scattering, *Phys. Rev. B* **61**, 9690 (2000).
- [49] G. C. Ménard, S. Guisart, C. Brun, R. T. Leriche, M. Trif, F. Debontridder, D. Demaille, D. Roditchev, P. Simon, and T. Cren, Two-dimensional topological superconductivity in Pb/Co/Si(111), *Nat. Commun.* **8**, 2040 (2017).

- [50] A. Palacio-Morales, E. Mascot, S. Cocklin, H. Kim, S. Rachel, D. K. Morr, and R. Wiesendanger, Atomic-scale interface engineering of Majorana edge modes in a 2D magnet-superconductor hybrid system, *Sci. Adv.* **5**, eaav6600 (2019).
- [51] S. Kezilebieke, M. N. Huda, V. Vaño, M. Aapro, S. C. Ganguli, O. J. Silveira, S. Głodzik, A. S. Foster, T. Ojanen, and P. Liljeroth, Topological superconductivity in a van der Waals heterostructure, *Nature (London)* **588**, 424 (2020).
- [52] S. Kezilebieke, V. Vaño, M. N. Huda, M. Aapro, S. C. Ganguli, P. Liljeroth, and J. L. Lado, Moiré - Enabled Topological Superconductivity, *Nano Lett.* **22**, 328 (2022).
- [53] D. Carvalho, N. A. García-Martínez, J. L. Lado, and J. Fernández-Rossier, Real-space mapping of topological invariants using artificial neural networks, *Phys. Rev. B* **97**, 115453 (2018).
- [54] J. F. Rodríguez-Nieva and M. S. Scheurer, Identifying topological order through unsupervised machine learning, *Nat. Phys.* **15**, 790 (2019).
- [55] N. L. Holanda and M. A. R. Griffith, Machine learning topological phases in real space, *Phys. Rev. B* **102**, 054107 (2020).
- [56] E. Lustig, O. Yair, R. Talmon, and M. Segev, Identifying Topological Phase Transitions in Experiments Using Manifold Learning, *Phys. Rev. Lett.* **125**, 127401 (2020).
- [57] P. Baireuther, M. Płodzień, T. Ojanen, J. Tworzydło, and T. Hyart, Identifying Chern numbers of superconductors from local measurements, [arXiv:2112.06777](https://arxiv.org/abs/2112.06777).
- [58] K. Pöyhönen, I. Sahlberg, A. Westström, and T. Ojanen, Amorphous topological superconductivity in a Shiba glass, *Nat. Commun.* **9**, 2103 (2018).
- [59] PYQULA Library <https://github.com/joselado/pyqula>.
- [60] T. Fukui, Y. Hatsugai, and H. Suzuki, Chern numbers in discretized Brillouin zone: Efficient method of computing (Spin) Hall conductances, *J. Phys. Soc. Jpn.* **74**, 1674 (2005).
- [61] F. Parisen Toldin, M. Hohenadler, F. F. Assaad, and I. F. Herbut, Fermionic quantum criticality in honeycomb and π -flux Hubbard models: Finite-size scaling of renormalization-group-invariant observables from quantum Monte Carlo, *Phys. Rev. B* **91**, 165108 (2015).
- [62] S.-S. Lee, Recent Developments in Non-Fermi Liquid Theory, *Annu. Rev. Condens. Matter Phys.* **9**, 227 (2018).
- [63] C. P. Moca, I. Weymann, M. A. Werner, and G. Zaránd, Kondo Cloud in a Superconductor, *Phys. Rev. Lett.* **127**, 186804 (2021).
- [64] R. Orús, A practical introduction to tensor networks: Matrix product states and projected entangled pair states, *Ann. Phys. (NY)* **349**, 117 (2014).
- [65] G. Carleo and M. Troyer, Solving the quantum many-body problem with artificial neural networks, *Science* **355**, 602 (2017).
- [66] A. Abouelkomsan, Z. Liu, and E. J. Bergholtz, Particle-Hole Duality, Emergent Fermi Liquids, and Fractional Chern Insulators in Moiré Flatbands, *Phys. Rev. Lett.* **124**, 106803 (2020).
- [67] C. Repellin and T. Senthil, Chern bands of twisted bilayer graphene: Fractional Chern insulators and spin phase transition, *Phys. Rev. Res.* **2**, 023238 (2020).
- [68] A. Georges, G. Kotliar, W. Krauth, and M. J. Rozenberg, Dynamical mean-field theory of strongly correlated fermion systems and the limit of infinite dimensions, *Rev. Mod. Phys.* **68**, 13 (1996).
- [69] G. Onida, L. Reining, and A. Rubio, Electronic excitations: Density-functional versus many-body Green's-function approaches, *Rev. Mod. Phys.* **74**, 601 (2002).
- [70] E. M. Stoudenmire, J. Alicea, O. A. Starykh, and M. P. A. Fisher, Interaction effects in topological superconducting wires supporting Majorana fermions, *Phys. Rev. B* **84**, 014503 (2011).